Journal of Magnetism and Magnetic Materials 453 (2018) 262–267

Contents lists available at ScienceDirect

Journal of Magnetism and Magnetic Materials

journal homepage: www.elsevier.com/locate/jmmm

Theoretical approach for determining the relation between the morphology and surface magnetism of Co_3O_4

R.A.P. Ribeiro [a], S.R. de Lazaro [a], L. Gracia [b], E. Longo [c], J. Andrés [d,*]

[a] Department of Chemistry, State University of Ponta Grossa, Av. General Carlos Cavalcanti, 4748, 84030-900 Ponta Grossa, PR, Brazil
[b] Department of Physical Chemistry, University of Valencia, 46100 Burjassot, Spain
[c] CDMF-UFSCar, Universidade Federal de São Carlos, PO Box 676, 13565–905 São Carlos, SP, Brazil
[d] Department of Analytical and Physical Chemistry, University Jaume I, Castelló 12071, Spain

ARTICLE INFO

Article history:
Received 2 October 2017
Received in revised form 27 October 2017
Accepted 6 November 2017
Available online 10 November 2017

Keywords:
Morphology
Wulff construction
Surface energy
Spin density
Magnetism
Co_3O_4

ABSTRACT

Precisely controlling the different aspects of the morphology and magnetic properties of metal oxides are fundamental to materials design. A theoretical approach, based on the Wulff construction and magnetization density (M) index, is presented to clarify the relation between the morphology and surface magnetism. The M index allows us to evaluate the uncompensated spins at the (1 0 0), (1 1 0), (1 1 1) and (1 1 2) surfaces of Co_3O_4 with a spinel structure. The investigated morphologies show an excellent agreement with the experimental results, with the main contribution coming from the (1 0 0) and (1 1 1) magnetic planes. The present results are also helpful in clarifying the intriguing magnetic properties reported for Co_3O_4 nanoparticles, suggesting that the same technique may serve as a guide for the study of shape-oriented magnetic materials.

1. Introduction

The functionality of nanomaterials is strongly related to their structure in terms of size and shape as well their corresponding electronic and spin densities, which are fundamental in controlling their nanoscopic, microscopic and macroscopic properties. Currently, remarkable advancements in a combination of theoretical and experimental techniques have allowed new functional materials to be designed as well as the main features behind nanostructures to be understood, enabling the enhancement of the performance of solid-state materials through morphological control. Indeed, kinds of applications such as catalysis, gas sensing, energy conversion and storage, and magnetoresistance depend on the atomic-level surface arrangement [1–4].

In recent years, many theoretical and experimental efforts have been dedicated to determining the morphologies of several metal oxides and explaining the existence of superior photocatalytic, photoluminescent and fungicidal activities. In general, such studies assume that morphological transformations are imposed by geometric constraints (dangling bonds, metals with low-coordination numbers, etc.), which control the surface energy. Then, the shape-oriented materials predicted *in silico* can be obtained *in situ* through the combination of different experimental techniques (synthetic methods, reaction times, surfactants and others) allowing the rational design of nanomaterials [2,5–17].

Recently, magnetic materials have attracted some interest because of the development of spintronic technologies and the revival of the discussion of multiferroic candidates. In this field, a large number of experimental studies have discussed the dependence of the surface morphology and unusual magnetic properties for different materials such as Co_3O_4, Mn_xO_y, Fe_xO_y, $CoFe_2O_4$ and MnS. Such shape-controlled nanoparticles exhibit different saturations, Neel temperatures and remanent magnetizations, showing a remarkable potential for technological applications involving high-density storage and processing devices [2,18–31]. However, from a theoretical point of view, it is well established that the atomic distributions control the spin coupling among unpaired electrons at the surface, and the relation between surface magnetism and morphology control remains unclear.

Co_3O_4 is a normal spinel (*Fd-3m* symmetry) that has been widely investigated because of its superior surface redox reactivity and electronic and magnetic properties, which have found several applications in energy conversion and storage, magnetic devices and catalysis. [32–34] The primary objective of this work was to demonstrate how the surface energies obtained from density functional theory calculations can be combined with the number of unpaired electrons per surface in order to determine the

* Corresponding author.
E-mail address: andres@qfa.uji.es (J. Andrés).

https://doi.org/10.1016/j.jmmm.2017.11.025
0304-8853/

magnetization of different morphologies. This theoretical approach is capable of finding a relationship between the magnetism of Co_3O_4 and the obtained morphologies under the equilibrium conditions of electronic and spin densities.

2. Theoretical method and computational procedure

In order to study the morphology, the classical Wulff construction is employed, which is based on the thermodynamic theory that the energy of the crystal facets (E_{surf}) determines the equilibrium morphology. The Wulff proposal refers to a simple relation between (E_{surf}) and the distance in the normal direction from the center of the crystallite, which also allows this ideal morphology to be modified by tuning the surface energies of the different facets [4,9,35,36].

In this work, we use the surface energy (E_{surf}) values calculated by Su et al. [27], where Density Functional Theory (DFT) calculations were performed employing LDA exchange-correlation functional and ultra-soft pseudopotential (USPP) formalism. The geometry of the (1 0 0), (1 1 0), (1 1 1), and (1 1 2) surfaces were described using the slab construction with thickness large enough to ensure full relaxation of the surface ions and convergence of the surface energy. In all cases, the atomic positions were relaxed using 0.001 eV as convergence criteria and the finite surface energy (E_{surf}) was calculated from the stoichiometric difference between the slab energy (E_{slab}) and the bulk energy (E_{bulk}) per unit area (A) [27].

What is new about this study is that the definition of the magnetization density ($\boldsymbol{D}_\mu$) index of a given surface is related with to the magnetic moment (μ_B) per unit cell area ($\boldsymbol{A}$):

$$\boldsymbol{D}_\mu = \frac{\mu_B}{\boldsymbol{A}} \tag{1}$$

$\boldsymbol{D}_\mu$ resembles the broken bonding density index proposed by Gao et al. and is widely used to clarify the nature of surface stability [37]. In addition, Beltrán et al. investigated the magnetic properties of cubic and tetragonal HfO_2 surfaces through a similar approach, which was helpful in clarifying the surface magnetization associated with vacancies and showed an excellent agreement with the experimental results [38–40].

Here, considering the magnetic ordering of the surfaces which is composed of different morphologies, we assume the $\boldsymbol{D}_\mu$ index can be used to classify the surfaces by following magnetic criteria. Therefore, from the combination of the polyhedral representation, $c_{(hkl)}$, derived from the Wulff construction and $\boldsymbol{D}_\mu$, it is possible to predict the total magnetization density ($\boldsymbol{M}$) index of a given morphology as follows:

$$\boldsymbol{M} = \sum \boldsymbol{c}_{(\boldsymbol{hkl})} \cdot \boldsymbol{D}_\mu^{(\boldsymbol{hkl})} \tag{2}$$

3. Results and discussion

The crystal structure of Co_3O_4 consists of a cubic close-packed array of oxygen anions where 1/8 of the tetrahedral interstices are occupied by high-spin Co^{2+} cations, while half the of octahedral interstices are occupied by low-spin Co^{3+} cations. Each Co^{2+} cation ($e_g^4t_{2g}^3$) is surrounded by four nearest neighbors of opposite spin, giving rise to an antiferromagnetic network. In contrast, the Co^{3+} cations exhibit a closed-shell configuration (t_{2g}^6) and nil magnetic moment, as depicted in Fig. 1.

The experimental and theoretical results indicate that the low index (1 0 0), (1 1 0), (1 1 1), and (1 1 2) surfaces control their morphology and can describe the structural arrangements commonly found in such materials [9,27,32,34,41]. In this case, considering the experimental antiferromagnetic arrangement-AFM (Fig. 1), each surface has a number of unpaired electrons per unit area, as depicted in Fig. 2 [42]. For instance, the (1 0 0) surface is composed of one Co^{2+} cation coordinated with two oxygen anions (Co_{2c}^{2+}) and five-coordinated Co^{3+} cations (Co_{5c}^{3+}) resulting in three unpaired electrons per unit surface area. Similarly, the (1 1 1) surface exhibits the same spin density as the (1 0 0) plane, being composed of one three-coordinated Co^{2+} cation (Co_{3c}^{2+}) and octahedral Co^{3+} cations (Co_{6c}^{3+}). In contrast, the (1 1 0) surface is formed by AFM planes containing two (Co_{3c}^{2+}) and (Co_{5c}^{3+}) cations, generating an antiparallel slab. In addition, some authors have reported that the (1 1 2) surface is more stable than the (1 1 1) surface, indicating that it can contribute to the morphology of the Co_3O_4 nanoparticles [9,27,43,44]. However, a deep analysis of the magnetic ordering along this plane reveals an antiparallel arrangement between two (Co_{3c}^{2+}) cations, resulting in an exposed plane with $\boldsymbol{D}_\mu = 0$ (Fig. 2). Especially for Co_3O_4, the understanding of the relation between the surface composition and its energy play a fundamental role in the clarification of the superior properties associated with the Co^{3+}/Co^{2+} ratio and the electronic and magnetic structure of such nanoparticles [45,46].

In this work, the Wulff construction for the Co_3O_4 structure was obtained from the surface energy (E_{surf}) values calculated by Su et al. [27] It is important to ascertain that such results are reason-

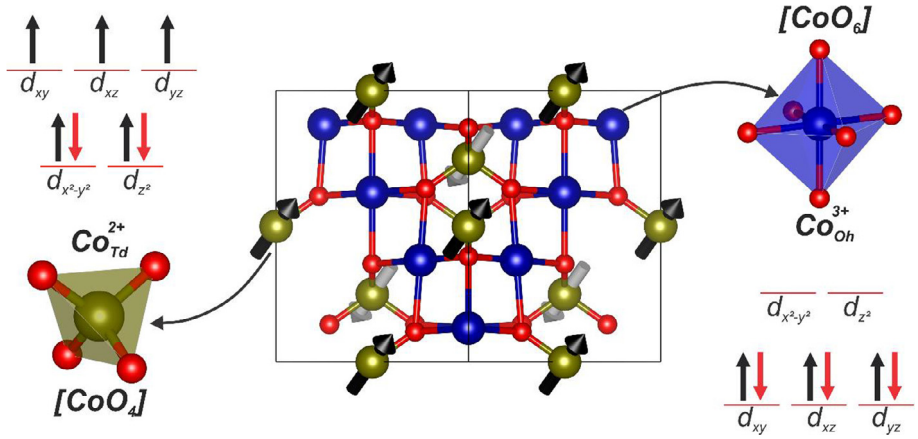

Fig. 1. Crystalline unit cell of Co_3O_4, local structures, and corresponding crystal field diagram for high-spin (HS) tetrahedral and low-spin (LS) octahedral cobalt atoms. The black and gray arrows indicate the up and down spin orientations following the experimental antiferromagnetic ordering. (For interpretation of the references to colour in this figure legend, the reader is referred to the web version of this article.)

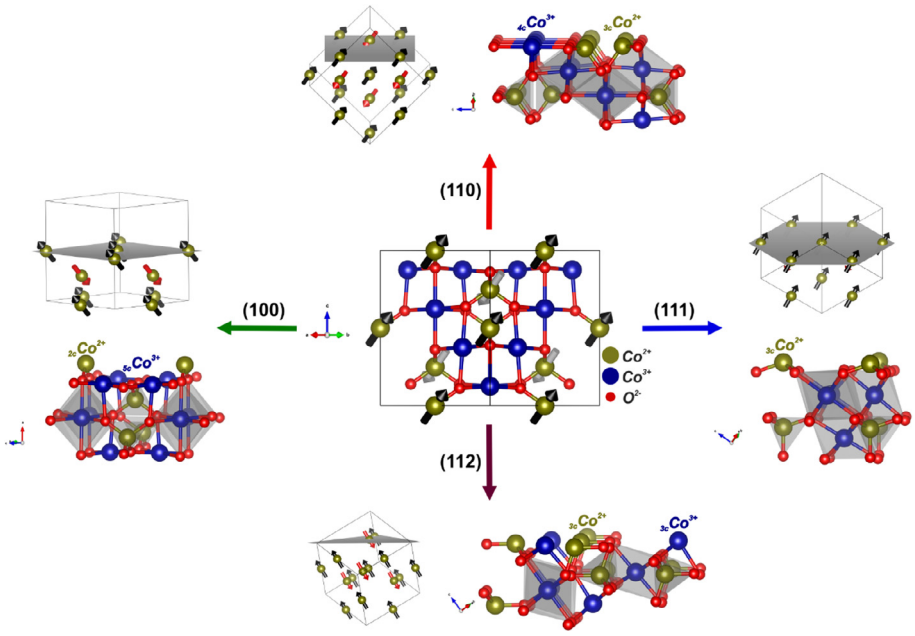

Fig. 2. Schematic representation of the unit cell of Co_3O_4 and its (1 0 0), (1 1 0), (1 1 1) and (1 1 2) surfaces. The black and grey arrows indicate the up and down spin orientations. (For interpretation of the references to colour in this figure legend, the reader is referred to the web version of this article.)

Table 1
Surface energy (E_{surf}), area (A), magnetic moment and magnetization density (D_μ) calculated for the Co_3O_4 spinel.

Surfaces	E_{surf} (J m^{-2})	A (nm^2)	Magnetic Moment (μ_b)	D_μ (μ_b nm^{-2})
(1 0 0)	0.92	0.33	3	9.21
(1 1 0)	1.31	0.46	0	0
(1 1 1)	2.31	0.28	3	10.64
(1 1 2)	1.46	0.80	0	0

able approximations to understand the physical and chemical properties of Co_3O_4 surfaces, though the stabilizing effects such as surface reconstructing and chemical adsorption could be helpful to clarify the superficial mechanisms. Table 1 summarizes the values of E_{surf}, μ_B, and D_μ of the surfaces used in the Wulff construction.

From Table 1, it is observed that the order of stability of the surfaces based on the energy criteria is (1 0 0) > (1 1 0) > (1 1 2) > (1 1 1). Furthermore, it is noted that both (1 0 0) and (1 1 1) surfaces exhibit similar values of unpaired electron densities along the slabs, while the (1 1 0) and (1 1 2) surfaces exhibit a zero magnetic moment along the plane.

Therefore, the computed surface energies induce a significant change in the equilibrium morphologies of Co_3O_4. The morphological modulations of Co_3O_4 proposed in this work are summarized in Fig. 3, in which the transformations are obtained by tuning the surface energies of the different facets.

The ideal morphology for Co_3O_4 predominantly exposes the (1 0 0) surface and, to a minor extent, the (1 1 2) surface, following the thermodynamic criteria from the values of the surface energies. In addition, it is observed that different shapes are obtained by tuning the E_{surf} for Co_3O_4 (Fig. 3). In the past few years, different strategies have been used to obtain different kinds of shape-oriented Co_3O_4 nanoparticles. For instance, Su et al. reported the synthesis of cubes and pseudo-octahedral Co_3O_4 nanoparticles, demonstrating an excellent agreement with theoretical morphologies 1 and 2.1, respectively. Especially, they argue that pseudo-octahedral nanocrystals expose the (1 0 0) and (1 1 0) planes, in which it is necessary to modify one of the (1 1 0)-surface groups ($E_{surf}^{(110)}$ can be $E_{surf}^{(110)}$, $E_{surf}^{(101)}$, $E_{surf}^{(011)}$) as described by Ferrer et al. [9,27] In contrast, Chen et al. and Dutta et al. synthesized a different kind of corner-truncated octahedral nanoparticle, which exposes the (1 0 0) and (1 1 1) surfaces, according to the theoretical morphology 3.2 [47,48]. They also report the existence of corner-truncated cubic shapes, which predominantly expose the (1 0 0) surface with different percentages of the (1 1 1) surface. A comparison and analysis of the morphologies reported by these authors with those found in our tree of morphologies, 3 and 3.1, show a great similarity [47]. Gao et al. studied the electrocatalytic performance of shape-oriented Co_3O_4 and reported the existence of octahedral shapes with the exposed (1 1 1) plane, corresponding to morphology 3.3 presented in Fig. 3 [49]. Moreover, Kang et al. revealed the shape evolution of Co_3O_4 nanocrystals and proved the existence of polyhedra with the exposed (1 0 0), (1 1 0), and (1 1 1) surfaces, which are in excellent agreement with morphology 2.3 [50]. It is important to clarify that Scanning Electron Microscopy (SEM) technique was employed to obtain the different morphologies reported by these authors [27,47–50]. In addition, several other authors reported similar shapes for Co_3O_4, showing that these nanoparticles exhibit a weak ferromagnetic ordering commonly attributed to the uncompensated spins obtained from the cleavage planes [18,21,48,51–57].

In order to relate the surface magnetism and morphology modulation of Co_3O_4, Table 2 presents the calculated surface area contributions for each polyhedron presented in Fig. 3, as well as the total magnetization density (M) index calculated by Eq. (2).

Regarding the uncompensated spin density for the different morphologies predicted for Co_3O_4, it is observed that higher M

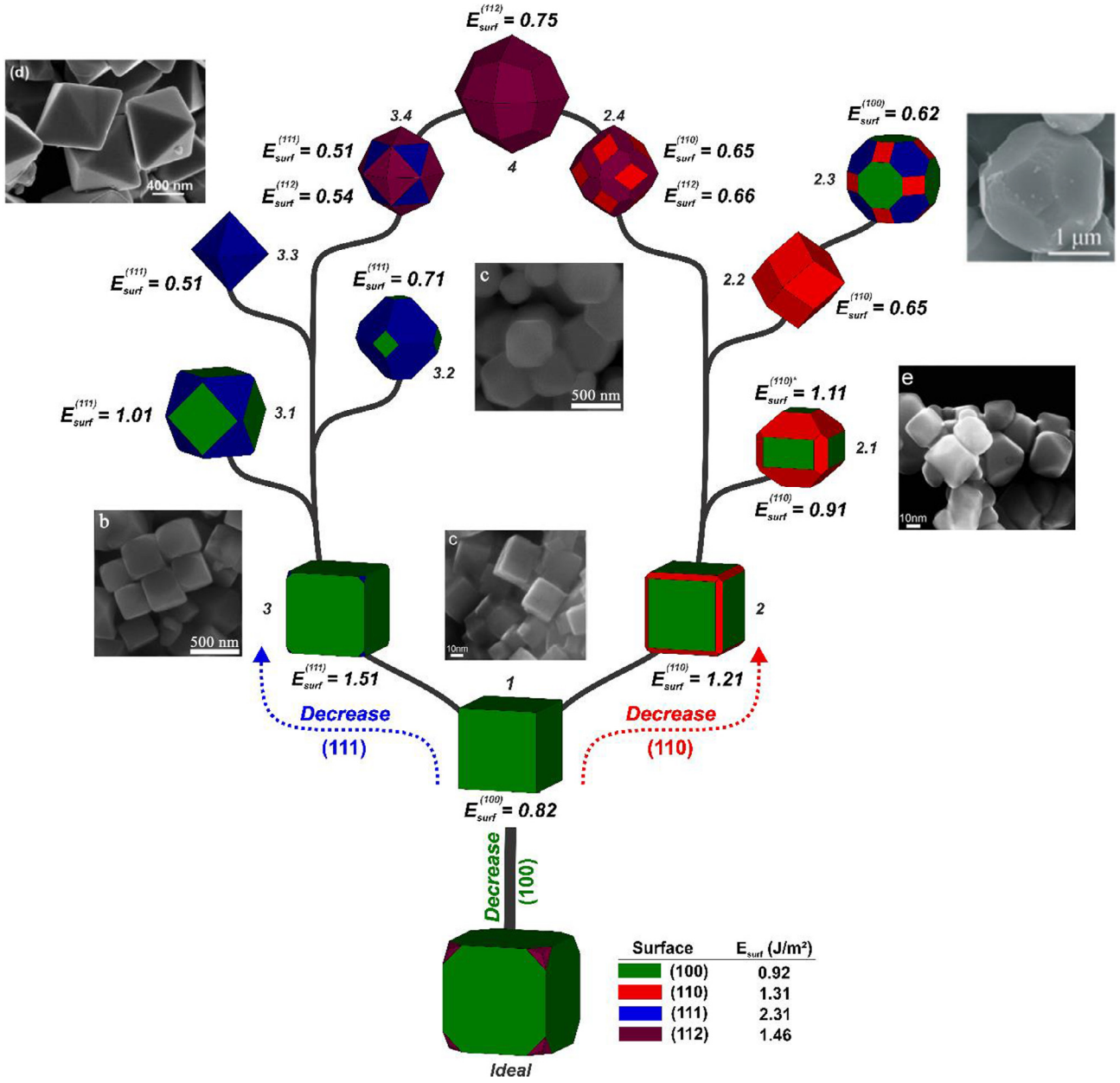

Fig. 3. Available morphologies for Co_3O_4 obtained from the (1 0 0), (1 1 0), (1 1 1) and (1 1 2) surface energies calculated by Su et al. [27] Reprinted by permission from Macmillan Publishers Ltd.: D. Su, S. Dou, G. Wang, Scientific Reports, vol. 4, 5767 (2014). Copyright 2014. Reproduced from Ref. [47] with permission from the PCCP Owner Societies. Reproduced from Ref. [50] with permission from The Royal Society of Chemistry. Reprinted with permission from R. Gao, J. Zhu, X. Xiao, Z. Hu, J. Liu, X. Liu, Facet-dependent electrocatalytic performance of Co_3O_4 for rechargeable Li-O2 battery. Copyright 2015 American Chemical Society. All experimental images were obtained using Scanning Electron Microscopy (SEM).

index values are obtained by tuning the contribution of the (1 0 0) and (1 1 1) surfaces, while the presence of (1 1 0) and (1 1 2) surfaces induces the smallest *M* index values. In addition, the experimental reports for the Co_3O_4 nanoparticles indicate that the (1 0 0) and (1 1 1) surfaces play a key role in the morphology transformations, indicating that the unpaired electron density contributes to the stabilization of shape-oriented nanoparticles. In this case, we can assume that the unusual magnetic properties related to the Co_3O_4 nanoparticles are related to the uncompensated spin density originating from the exposition of magnetic planes found along the AFM ordering.

From the analysis of the results reported in Table 2, it is possible to propose a different kind of morphology map, based on the combination of E_{surf} and *M* values. In this case, we only consider the (1 0 0) and (1 1 1) planes, which exhibit non-zero values of the magnetic moment. The modulation process associated with the change of morphology is depicted in the schema in Fig. 4. Regular/truncated cubes and octahedral shapes with exposed (1 0 0) and (1 1 1) surfaces are observed, respectively. The increase in magnetization as the E_{surf} values of the (1 1 1) surface decreases can be explained by the surface spin disorder of the Co_3O_4 particles being more easily aligned in the direction of the core spins via the applied magnetic field. Indeed, experimental results for Co_3O_4 nanoparticles suggest the relation between crystal size/shape and its magnetism arguing that the increased ferromagnetic component is associated with the magnetic moments on the magnetic sublattices, which do not cancel out completely. In such studies, the authors report the presence of cubic, regular and

Table 2
Surface contribution and total magnetization density (M) index calculated for Co_3O_4.

Morphology	Surface contribution (%)				M (u_b nm^{-2})
	(1 0 0)	(1 1 0)	(1 1 1)	(1 1 2)	
Ideal	99	–	–	1	9.12
1.0	100	0.00	–	–	9.21
2.0	89	11	–	–	8.20
2.1	52	48	–	–	4.80
2.2	–	100	–	–	0
2.3	50	13	37	–	8.58
2.4	–	48	–	52	0
3.0	99	–	1.0	–	9.22
3.1	61	–	39	–	9.76
3.2	15	–	85	–	10.42
3.3	–	–	100	–	10.63
3.4	–	–	58	42	6.17
4.0	–	–	–	100	0

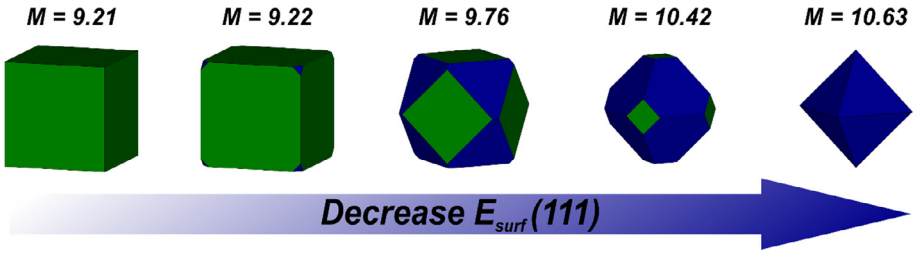

Fig. 4. Morphology modulation based on the combination of values for the surface energy (E_{surf}) and total magnetization density (M) for Co_3O_4.

truncated-octahedral morphologies showing an excellent agreement with theoretical polyhedrons depicted in Fig. 4, indicating that ferromagnetic (1 0 0) and (1 1 1) planes play a fundamental role on the unusual magnetism of Co_3O_4 nanoparticles [48,55].

It is important to note that the incorporation of the total magnetization density, M index, along the Wulff construction produces a particular variety of morphologies that coincide with the experimental modulations found for the Co_3O_4 nanoparticles [27,47,49,50]. The geometric constraints imposed by the morphology map, obtained by the Wulff construction, are modified when the magnetic surfaces are considered through a reorientation of the crystalline structure which induces a different spin distribution along the material surfaces. Thus, we can argue that such procedures can be used as a guide for the theoretical/experimental study of shape-oriented magnetic nanoparticles.

4. Conclusions

A novel approach was proposed to analyze the magnetic properties of shape-controlled materials. This procedure combines the Wulff construction and the values of spin density to predict the morphology while considering the uncompensated spins for magnetic materials. By controlling the ratio of the surface energy values, a complete set of morphologies for Co_3O_4 were predicted, showing an excellent agreement with the experimental results. In addition, the reported results confirm that such morphologies have a singular spin density along the exposed area, which is helpful for understanding the unusual magnetic deviations commonly found for Co_3O_4 nanoparticles. From the viewpoint of applications, the ability to produce Co_3O_4 nanoparticles with high magnetization is highly desirable. Therefore, the present work on Co_3O_4 magnetic materials *in silico* can be directly related to the experimental findings, and can lead to innovation of the materials design through multifunctional shape-oriented nanoparticles. Based on these results and the facts reported in the literature, we can conclude that controlling the crystallinity and the exposed surface of the nanoparticles, it is possible to influence the magnetization properties of Co_3O_4 nanoparticles.

Acknowledgments

This work was supported by the State University of Ponta Grossa, Universitat Jaume I, CAPES and Araucaria Foundation. J.A. acknowledges the financial support of the following agencies: Generalitat Valenciana for PrometeoII/2014/022, Prometeo/2016/079, ACOMP/2014/270, ACOMP/2015/1202, Ministerio de Economia y Competitividad, project CTQ2015-65207-P.

References

[1] A. Seyed-Razavi, I.K. Snook, A.S. Barnard, Origin of nanomorphology: does a complete theory of nanoparticle evolution exist?, J Mater. Chem. 20 (2010) 416–421.
[2] Y. Xia, X. Xia, H.-C. Peng, Shape-controlled synthesis of colloidal metal nanocrystals: thermodynamic versus kinetic products, J. Am. Chem. Soc. 137 (2015) 7947–7966.
[3] S.J.L. Billinge, I. Levin, The problem with determining atomic structure at the nanoscale, Science 316 (2007) 561–565.
[4] G.D. Barmparis, Z. Lodziana, N. Lopez, I.N. Remediakis, Nanoparticle shapes by using Wulff constructions and first-principles calculations, Beilstein J. Nanotechnol. 6 (2015) 361–368.
[5] M.R.D. Bomio, R.L. Tranquilin, F.V. Motta, C.A. Paskocimas, R.M. Nascimento, L. Gracia, J. Andres, E. Longo, Toward understanding the photocatalytic activity of $PbMoO_4$ powders with predominant (111), (100), (011), and (110) facets. A Combined Experimental and Theoretical Study, J. Phys. Chem. C 117 (2013) 21382–21395.
[6] G. Botelho, J. Andres, L. Gracia, L.S. Matos, E. Longo, Photoluminescence and photocatalytic properties of Ag_3PO_4 microcrystals: an experimental and theoretical investigation, ChemPlusChem 81 (2016) 202–212.
[7] G. Byzynski, C. Melo, D.P. Volanti, M.M. Ferrer, A.F. Gouveia, C. Ribeiro, J. Andrés, E. Longo, The interplay between morphology and photocatalytic activity in ZnO and N-doped ZnO crystals, Mater. Des. 120 (2017) 363–375.
[8] R.C. de Oliveira, C.C. de Foggi, M.M. Teixeira, M.D.P. da Silva, M. Assis, E.M. Francisco, B.N.A.d.S. Pimentel, P.F.d.S. Pereira, C.E. Vergani, A.L. Machado, J. Andres, L. Gracia, E. Longo, Mechanism of antibacterial activity via morphology change of α-$AgVO_3$: theoretical and experimental Insights, ACS Appl. Mater. Interfaces 9 (2017) 11472–11481.
[9] M.M. Ferrer, A.F. Gouveia, L. Gracia, E. Longo, J. Andrés, A 3D platform for the morphology modulation of materials: first principles calculations on the

thermodynamic stability and surface structure of metal oxides: Co3O4, α-Fe2O3, and In2O3, Modell. Simul. Mater. Sci. Eng. 24 (2016).
[10] A.F. Gouveia, M.M. Ferrer, J.R. Sambrano, J. Andrés, E. Longo, Modeling the atomic-scale structure, stability, and morphological transformations in the tetragonal phase of $LaVO_4$, Chem. Phys. Lett. 660 (2016) 87–92.
[11] F.A. La Porta, A.E. Nogueira, L. Gracia, W.S. Pereira, G. Botelho, T.A. Mulinari, J. Andrés, E. Longo, An experimental and theoretical investigation on the optical and photocatalytic properties of ZnS nanoparticles, J. Phys. Chem. Solids 103 (2017) 179–189.
[12] V.M. Longo, L. Gracia, D.G. Stroppa, L.S. Cavalcante, M. Orlandi, A.J. Ramirez, E. R. Leite, J. Andrés, A. Beltrán, J.A. Varela, E. Longo, A joint experimental and theoretical study on the nanomorphology of $CaWO_4$ crystals, J. Phys. Chem. C 115 (2011) 20113–20119.
[13] M.C. Oliveira, L. Gracia, M. de Assis, I.L.V. Rosa, M.F. do Carmo Gurgel, E. Longo, J. Andrés, Mechanism of photoluminescence in intrinsically disordered $CaZrO_3$ crystals: first principles modeling of the excited electronic states, J. Alloy. Compd. 722 (2017) 981–995.
[14] M.C. Oliveira, L. Gracia, I.C. Nogueira, M.F.D. Carmo Gurgel, J.M.R. Mercury, E. Longo, J. Andrés, Synthesis and morphological transformation of $BaWO_4$ crystals: experimental and theoretical insights, Ceram. Int. (2016).
[15] P.F.S. Pereira, C.C. Santos, A.F. Gouveia, M.M. Ferrer, I.M. Pinatti, G. Botelho, J.R. Sambrano, I.L.V. Rosa, J. Andrés, E. Longo, α-$Ag_{2-2x}Zn_xWO_4$ ($0 \leq x \leq 0.25$) Solid solutions: structure, morphology, and optical properties, Inorg. Chem 56 (2017) 7360–7372.
[16] R.A. Roca, P.S. Lemos, L. Gracia, J. Andrés, E. Longo, Uncovering the metastable γ-Ag_2WO4 phase: a joint experimental and theoretical study, RSC Adv. 7 (2017) 5610–5620.
[17] D.G. Stroppa, L.A. Montoro, A. Campello, L. Gracia, A. Beltrán, J. Andrés, E.R. Leite, A.J. Ramirez, Prediction of dopant atom distribution on nanocrystals using thermodynamic arguments, Phys. Chem. Chem. Phys. 16 (2014) 1089–1094.
[18] G. Anandha Babu, G. Ravi, Y. Hayakawa, M. Kumaresavanji, Synthesis and calcinations effects on size analysis of Co_3O_4 nanospheres and their superparamagnetic behaviors, J. Magn. Magn. Mater. 375 (2015) 184–193.
[19] P. Guo, G. Zhang, J. Yu, H. Li, X.S. Zhao, Controlled synthesis, magnetic and photocatalytic properties of hollow spheres and colloidal nanocrystal clusters of manganese ferrite, Colloids Surfaces A: Physicochem. Eng. Aspects 395 (2012) 168–174.
[20] D. Jagadeesan, U. Mansoori, P. Mandal, A. Sundaresan, M. Eswaramoorthy, Hollow spheres to nanocups: tuning the morphology and magnetic properties of single-crystalline α-Fe_2O_3 nanostructures, Angew. Chem. Int. Ed. 47 (2008) 7685–7688.
[21] Y.W. Jun, Y.Y. Jung, J. Cheon, Architectural control of magnetic semiconductor nanocrystals, J. Am. Chem. Soc. 124 (2002) 615–619.
[22] D. Liu, X. Wang, X. Wang, W. Tian, Y. Bando, D. Golberg, Co_3O_4 nanocages with highly exposed {110} facets for high-performance lithium storage, Sci. Rep. 3 (2013) 2543.
[23] J. Ma, J. Lian, X. Duan, X. Liu, W. Zheng, α-Fe_2O_3: hydrothermal synthesis, magnetic and electrochemical properties, J. Phys. Chem. C 114 (2010) 10671–10676.
[24] D.T. Margulies, F.T. Parker, F.E. Spada, R.S. Goldman, J. Li, R. Sinclair, A.E. Berkowitz, Anomalous moment and anisotropy behavior in Fe_3O_4 films, Phys. Rev. B – Condens. Matter Mater. Phys. 53 (1996) 9175–9187.
[25] S. Mitra, S. Das, K. Mandal, S. Chaudhuri, Synthesis of a α-Fe_2O_3 nanocrystal in its different morphological attributes: growth mechanism, optical and magnetic properties, Nanotechnology 18 (2007).
[26] Q. Song, Z.J. Zhang, Shape control and associated magnetic properties of spinel cobalt ferrite nanocrystals, J. Am. Chem. Soc. 126 (2004) 6164–6168.
[27] D. Su, S. Dou, G. Wang, Single crystalline Co_3O_4 nanocrystals exposed with different crystal planes for Li-O_2 batteries, Sci. Rep. 4 (2014).
[28] A.S. Teja, P.-Y. Koh, Synthesis, properties, and applications of magnetic iron oxide nanoparticles, Prog. Cryst. Growth Charact. Mater. 55 (2009) 22–45.
[29] X. Wang, L. Yu, X.L. Wu, F. Yuan, Y.G. Guo, Y. Ma, J. Yao, Synthesis of single-crystalline Co_3O_4 octahedral cages with tunable surface aperture and their lithium storage properties, J. Phys. Chem. C 113 (2009) 15553–15558.
[30] J. Xiao, Q. Kuang, S. Yang, F. Xiao, S. Wang, L. Guo, Surface structure dependent electrocatalytic activity of Co_3O_4 anchored on graphene sheets toward oxygen reduction reaction, Sci. Rep. 3 (2013).
[31] X.L. Xu, Z.H. Chen, Y. Li, W.K. Chen, J.Q. Li, Bulk and surface properties of spinel Co_3O_4 by density functional calculations, Surf. Sci. 603 (2009) 653–658.
[32] X. Wang, W. Tian, T. Zhai, C. Zhi, Y. Bando, D. Golberg, Cobalt(II, III) oxide hollow structures: fabrication, properties and applications, J. Mater. Chem. 22 (2012) 23310–23326.
[33] J.M. Xu, J.P. Cheng, The advances of Co_3O_4 as gas sensing materials: a review, J. Alloy. Compd. 686 (2016) 753–768.
[34] H. Sun, H.M. Ang, M.O. Tade, S. Wang, Co_3O_4 nanocrystals with predominantly exposed facets: synthesis, environmental and energy applications, J. Mater. Chem. A 1 (2013) 14427–14442.
[35] T.L. Einstein, 5 - Equilibrium Shape of Crystals A2 – Nishinaga, Tatau, in: Handbook of Crystal Growth, Second Ed., Elsevier, Boston, 2015, pp. 215–264.
[36] The Wulff theorem, in: The Wulff Crystal in Ising and Percolation Models: Ecole d'Eté de Probabilités de Saint-Flour XXXIV - 2004, Springer Berlin Heidelberg, Berlin, Heidelberg, 2006, pp. 189–199.
[37] Z.-Y. Gao, W. Sun, Y.-H. Hu, Mineral cleavage nature and surface energy: anisotropic surface broken bonds consideration, Trans. Nonferrous Metals Soc. China 24 (2014) 2930–2937.
[38] J.M.D. Coey, High-temperature ferromagnetism in dilute magnetic oxides, J. Appl. Phys. 97 (2005) 10D313.
[39] J.M.D. Coey, M. Venkatesan, P. Stamenov, C.B. Fitzgerald, L.S. Dorneles, Magnetism in hafnium dioxide, Phys. Review B 72 (2005) 024450.
[40] J.I. Beltrán, M.C. Muñoz, J. Hafner, Structural, electronic and magnetic properties of the surfaces of tetragonal and cubic HfO_2, New J. Phys. 10 (2008) 063031.
[41] F. Zasada, W. Piskorz, P. Stelmachowski, A. Kotarba, J.F. Paul, T. Płociński, K.J. Kurzydłowski, Z. Sojka, Periodic DFT and HR-STEM studies of surface structure and morphology of cobalt spinel nanocrystals. Retrieving 3D shapes from 2D images, J. Phys. Chem. C 115 (2011) 6423–6432.
[42] S. Thota, S. Singh, Nature of magnetic ordering in cobalt-based spinels, in: M.S. Seehra (Ed.), Magnetic Spinels – Synthesis, Properties and Applications, InTech, Rijeka, 2017, p. 04.
[43] L. Hu, Q. Peng, Y. Li, Selective synthesis of Co_3O_4 nanocrystal with different shape and crystal plane effect on catalytic property for methane combustion, J. Am. Chem. Soc. 130 (2008) 16136–16137.
[44] R. Wei, X. Zhou, T. Zhou, J. Hu, J.C. Ho, Co3O4 nanosheets with in-plane pores and highly active 112 exposed facets for high performance lithium storage, J. Phys. Chem. C 121 (2017) 19002–19009.
[45] J. Wang, R. Gao, D. Zhou, Z. Chen, Z. Wu, G. Schumacher, Z. Hu, X. Liu, Boosting the electrocatalytic activity of Co_3O_4 nanosheets for a Li-O_2 battery through modulating inner oxygen vacancy and exterior Co^{3+}/Co^{2+} ratio, ACS Catal. (2017) 6533–6541.
[46] S.C. Petitto, E.M. Marsh, G.A. Carson, M.A. Langell, Cobalt oxide surface chemistry: the interaction of CoO(100), Co_3O_4 (110) and Co_3O_4 (111) with oxygen and water, J. Mol. Catal. A: Chem. 281 (2008) 49–58.
[47] Z. Chen, C.X. Kronawitter, B.E. Koel, Facet-dependent activity and stability of Co_3O_4 nanocrystals towards the oxygen evolution reaction, Phys. Chem. Chem. Phys. 17 (2015) 29387–29393.
[48] P. Dutta, M.S. Seehra, S. Thota, J. Kumar, A comparative study of the magnetic properties of bulk and nanocrystalline Co_3O_4, J. Phys.: Condens. Matter 20 (2008) 015218.
[49] R. Gao, J. Zhu, X. Xiao, Z. Hu, J. Liu, X. Liu, Facet-dependent electrocatalytic performance of Co_3O_4 for rechargeable Li-O_2 battery, J. Phys. Chem. C 119 (2015) 4516–4523.
[50] M. Kang, H. Zhou, D. Wu, B. Lv, Systematic shape evolution of Co_3O_4 nanocrystals from octahedra to spheres under the influence of $C_2O_4^{2-}$ and PVP, CrystEngComm 18 (2016) 9299–9306.
[51] M. Mansournia, N. Rakhshan, Amine ligand-based hydrothermal synthesis of Co_3O_4 nanoparticles, characterization and magnetic study, J. Mol. Struct. 1125 (2016) 714–720.
[52] A.S. Bhatt, D.K. Bhat, C.W. Tai, M.S. Santosh, Microwave-assisted synthesis and magnetic studies of cobalt oxide nanoparticles, Mater. Chem. Phys. 125 (2011) 347–350.
[53] T. Ozkaya, A. Baykal, M.S. Toprak, Y. Koseoğlu, Z. Durmuş, Reflux synthesis of Co_3O_4 nanoparticles and its magnetic characterization, J. Magn. Magn. Mater. 321 (2009) 2145–2149.
[54] D. Driele von, P. Ernesto Chaves, O. Adilson Jesus Aparecido de, Observation of superficial antiferromagnetism in Co_3O_4 polycrystals, Mater. Res. Express 2 (2015) 116102.
[55] T. Mousavand, T. Naka, K. Sato, S. Ohara, M. Umetsu, S. Takami, T. Nakane, A. Matsushita, T. Adschiri, Crystal size and magnetic field effects in Co_3O_4 antiferromagnetic nanocrystals, Phys. Rev. B 79 (2009) 144411.
[56] V. Bisht, K.P. Rajeev, Non-equilibrium effects in the magnetic behavior of Co_3O_4 nanoparticles, Solid State Commun. 151 (2011) 1275–1279.
[57] A. Tomou, D. Gournis, I. Panagiotopoulos, Y. Huang, G.C. Hadjipanayis, B.J. Kooi, Weak ferromagnetism and exchange biasing in cobalt oxide nanoparticle systems, J. Appl. Phys. 99 (2006) 123915.